Electrochemistry Communications 40 (2014) 54–57

Contents lists available at ScienceDirect

Electrochemistry Communications

journal homepage: www.elsevier.com/locate/elecom

Short communication

Interconnected carbon-decorated Tio_2 nanocrystals with enhanced lithium storage performance

Yuanyuan Zhou [a], Songhun Yoon [b,*]

[a] School of Engineering, Brown University, Providence, RI 02912, United States
[b] School of Integrative Engineering, Chung-Ang University, Heuksukdong 84, Dongjakgu 156-756, South Korea

ARTICLE INFO

Article history:
Received 6 November 2013
Received in revised form 12 December 2013
Accepted 20 December 2013
Available online 29 December 2013

Keywords:
TiO_2
Anode
Lithium ion batteries

ABSTRACT

A novel direct preparation method was developed to prepare interconnected carbon-decorated TiO_2 nanocrystals. The as-prepared composite exhibited a morphology of interconnected 10 nm TiO_2 nanocrystals with uniform carbon coverage. As anode in lithium ion batteries, high reversible capacity of 184 mAh g^{-1} with 87.4% initial coulomb efficiency, outstanding rate performance and stable cycle life were observed, which was attributed to ultrafine particle size, uniform carbon coating and high preparation temperature.

1. Introduction

Enormous efforts have been recently made to develop high performance anode materials for next generation lithium ion batteries (LIBs) [1–3]. Nanostructured titania with various polymorphs and morphologies have been considered as promising candidates because of its fast lithium insertion/deinsertion kinetics, high operating voltage, reliable safety, non-toxicity and low cost [4–7]. However, some shortcomings such as crystal aggregation during cycling and limited electric conductivity have been observed in the pure nanostructured TiO_2 anodes [8,9]. In order to overcome these obstacles, carbon-coated titania nanostructures have been widely investigated and performance improvement as anodes in LIBs has been observed [8–10]. TiO_2 micro-/nano-structure was first prepared and subsequent composite formation between TiO_2 and carbon phase was then conducted. Similar methods such as mechanical ball milling with graphite and post-pyrolysis of carbon precursors have been employed. However, it is unavoidable that these two-step methods are complicated and time-consuming [11–13]. Although one-step hydrothermal route was tried [25], the titania precursors were sensitive to moisture and reproducibility of preparation may be concerned. Hence, facile one-step method using stable precursors is highly required. Furthermore, performance of TiO_2 anode was reported to depend on the preparation temperature [6]. With low-temperature heat-treatment (<500 °C), distorted crystal lattice and deleterious surface functional groups can exist in TiO_2. These problems result in highly irreversible Li^+ consumption during the first lithiation process and low initial coulomb efficiency (IE) is unavoidable [6]. For the purpose of IE improvement, calcination temperature should be as high as possible, which usually brings about crystal aggregation and coarsening of TiO_2 [6].

Herein, we propose a direct preparation of novel TiO_2–C nanocomposite starting from an environment-friendly and moisture-insensitive precursors, namely interconnected carbon-decorated titania nanocrystals (CDTN). In our novel preparation, highly crystalline TiO_2 nanoparticles with uniform carbon coating survived even after high calcination temperature. Following advantageous features are expected in CDTN anode: i) ultrafine nano-TiO_2 crystals possess enhanced lithium uptake capability; ii) uniformly decorated carbon phase makes an improved electrical conductive network; iii) carbon phase avoids the direct contact between individual titania crystals, thus preventing crystal aggregation during battery cycling; iv) highly developed TiO_2 crystal structure with complete removal of surface functional groups ensures an improved IE.

2. Experimental

2.1. Preparation of the interconnected carbon-decorated titania nanocrystals (CDTN)

Self-made resol oligomers ($Mw < 500$) and titanium citrate complex solution were prepared according to reported method [10,15]. Typically, 4 g of 20 wt.% resol ethanol solution and 6 ml of 0.5 M titanium citrate complex ethanol solution was added dropwise into 8 g of ethanol under stirring. After stirring for 2 h, orange solution was poured into a big dish and kept in the ambient environment. After complete solvent evaporation, the dish was transferred into the oven at 100 °C for 24 h and a polymeric film was acquired. The film was carbonized at 750 °C for 2 h (the temperature ramping rate is 5 °C min^{-1}). As soon as the temperature was cooled down to the room temperature, the carbonized

* Corresponding author.
E-mail address: yoonshun@cau.ac.kr (S. Yoon).

1388-2481/$ – see front matter
http://dx.doi.org/10.1016/j.elecom.2013.12.028

sample was ground into fine powders and indexed as carbon–TiO_2 composite (CT). Then, the CT sample was calcinated at 450 °C for 30 m in air (the temperature ramping rate is 6 °C min^{-1}) to produce CDTN.

2.2. Characterization and anode performance investigation

The X-ray diffraction (XRD) patterns were obtained with a Rigaku D/Max-3C diffractometer equipped with a rotating anode and Cu K_α radiation ($\lambda = 0.15418$ nm). The external morphology of materials was examined using a scanning electron microscope (SEM, Philips XL30S FEG), whereas the pore images were obtained by a transmission electron microscope (TEM, TECNAI G2 T-20S). The anode performance was analyzed with a coin-type (CR2016) two-electrode cell with Li foil counter electrode (Cyprus Co.) and electrolyte of 1.0 M $LiPF_6$ in ethylene carbonate (EC)/dimethyl carbonate (DMC) (1:1 volume ratio) (Techno Semichem). The galvanostatic charge–discharge testing with a voltage range of 1.0–2.5 V *vs.* Li/Li^+ was conducted at the current rate from 0.2C to 10C (1C was in our experiments defined as 150 mA g^{-1}) on a WBCS-3000 battery cycler (WonATech) at ambient temperature. The cycle performance for 100 cycles was recorded at 0.2C. Cyclic voltammetry was measured on IviumStat Electrochemical Interface (Ivium Technologies) with a voltage range of 1.0–2.5 V *vs.* Li/Li^+ at 0.2 mV s^{-1}.

3. Results and discussion

Fig. 1 schematically shows formation process of the CDTN material. The resol oligomers and titanium citrate complex are initially dispersed in the ethanol and interacted each other. With process of ethanol-evaporation, polymerization and carbonization, a carbon–TiO_2 nanocomposite (CT) with ~60 wt.% carbon is obtained. Afterward, CT is carefully calcinated under air, which produces interconnected carbon-decorated TiO_2 nanocrystals (CDTN). The selection of precursors plays a key role for successful synthesis of CDTN. Titanium citrate complex, with a special cage-like titanium-centered complex molecular structure, strongly interacts and crosslinks with resols to form Ti-containing hybrid polymer [10,14–16], which probably retards organic–inorganic phase separation. Isolated Ti-containing nanophases can be homogeneously located within the resol polymeric matrix [14,15]. With calcination in nitrogen and air atmosphere sequentially, the Ti-containing nanophases are converted into ultrafine TiO_2 nanoparticles, while carbon derived from the resol polymer can coat on the TiO_2 surface. Because of strong confinement of these isolated Ti phases, fine nanostructure survives even after high-temperature heat-treatment.

In Fig. 2(a), TEM images of CT material show that high-contrast nanocrystals were uniformly dispersed in low-contrast carbon phase. In CDTN, morphology became mesoporous structure after carbon burning as shown in Fig. 2(b). From high resolution TEM images in Fig. 2(c) and (d), estimated TiO_2 crystal size was 5 and 10 nm for CT and CDTN, respectively, which coincided with average crystal size estimated by XRD patterns in Fig. 2(f) [17]. This indicated that fine titania nanocrystals formed in the initial step and severe crystal coarsening was effectively prohibited in CDTN. As shown in Fig. 2(f), main titania phase in both samples was anatase while rutile and brookite phase appeared as minor ones, which is associated with further heating process. In Fig. 2(e), SEM analysis shows external morphology of stacked TiO_2 nanoparticles in CDTN, implying that interstitial spaces between nanoparticles generated mesopores. Also, the inset EDS mapping demonstrated that

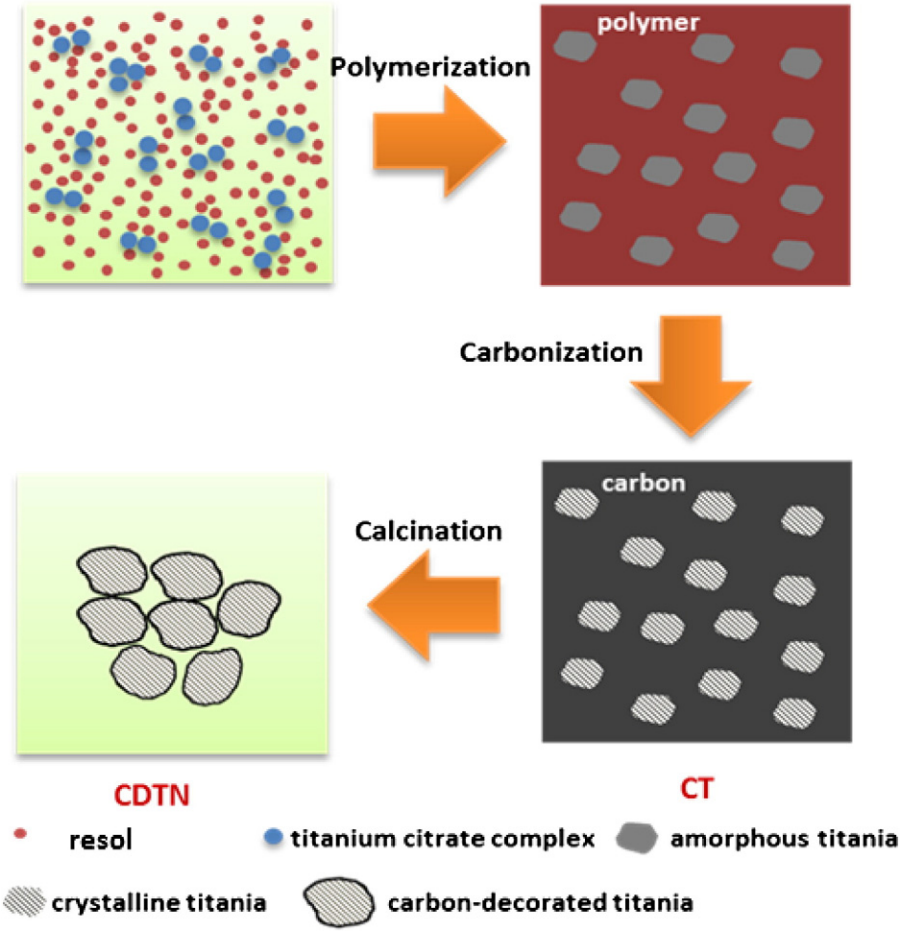

Fig. 1. Scheme of direct synthesis of the interconnected carbon-decorated titania nanocrystals (CDTN).

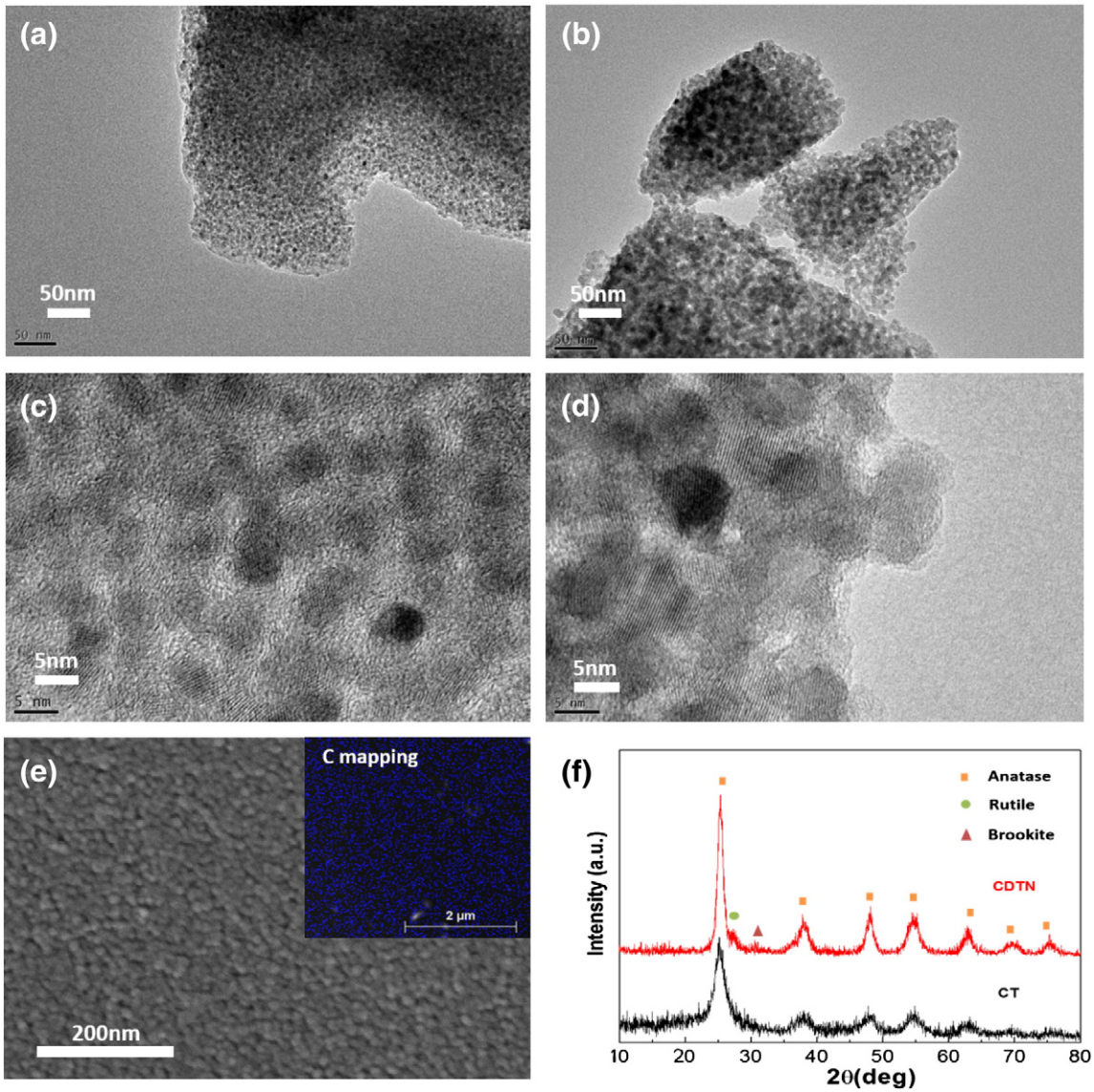

Fig. 2. TEM images of CT (a) and CDTN (b); High-resolution TEM images of CT (c) and CDTN (d); (e) SEM image of CDTN and EDX element mapping of carbon; (f) XRD patterns of the CT and CDTN.

carbon uniformly covered the surface of the interconnected titania nanocrystals. From our preliminary TGA and EDS experiments, estimated carbon fraction in CDTN was less than 3 wt.%, indicating that lithium storage contribution within the carbon structure can be negligible. From N_2 sorption isotherm, furthermore, CDTN exhibited typical mesoporous structure with BET surface area of 57 $m^2\ g^{-1}$ and the mean pore size was 4.7 nm, which was related to the interstitial space from the nanoparticles close packing. After preparation, anode performance of CDTN was investigated.

Fig. 3(a) shows the initial galvanostatic charge–discharge profiles of CDTN anode at the rate of 0.2C. As seen, surprisingly, the reversible capacity was as high as 184 mAh g^{-1} (0.55 mole Li^+ per 1 mole TiO_2; $Li_{0.55}TiO_2$), which is higher than the highest anode capacity of bulk anatase TiO_2 materials ($Li_{0.5}TiO_2$, 168 mAh g^{-1}) [6]. The core-shell anatase TiO_2–C nanocomposite with particle size of about 100 nm exhibited a capacity of only 122 mAh g^{-1} [9]. The self-assembled anatase–graphene with 2.5 wt.% graphene displayed similar capacity with CDTN (~180 mAh g^{-1}) [26]. Hence, CDTN anode exhibited one of the highest capacities in spite of much easier preparation route. This lithium storage enhancement in CDTN was certainly attributed to facile Li^+ uptake within the uniform TiO_2 nanoparticles and additional lithium storage at nanosized rutile and brookite phase (see Fig. 2(f)) [19,20]. Interestingly, the galvanostatic charge–discharge profiles of the CDTN anode were very similar to the mesoporous anatase TiO_2, indicative of a similar lithium-storage mechanism [21]. The IE of CDTN anode is as high as 87.4%, which was higher than the mesoporous anatase TiO_2 (less than 80%), the mesoporous TiO_2–carbon nanocomposites [15,18,21,22] and anatase–graphene nanocomposites (<70%) [26,27]. This very high IE in CDTN was certainly ascribed to complete removal of the detrimental functional groups and species on the surface after high temperature calcination at 750 °C.

Fig. 3 (b) shows cyclic voltammogram of CDTN anode from 1st to 4th cycle. Redox peaks pair near 2 V *vs.* Li/Li^+ corresponded to the voltage plateau in the galvanostatic charge–discharge profiles as shown in Fig. 3(a). The peaks pair was consistent with the anatase anodes, reflecting Li^+ was mostly stored by diffusion into the octahedral interstitial sites [13]. Note that the peak broadening was possibly due to nanosize effect, which was also observed in the hollow structured anatase [23,24]. Fig. 3(c) shows the rate performance of CDTN anode at the current density from 0.2C to 10C rate. As seen, rate capability of CDTN was outstanding (57% at 10C, actual current density was 1.5 A g^{-1}), which is probably ascribed to the high electrical conductivity by

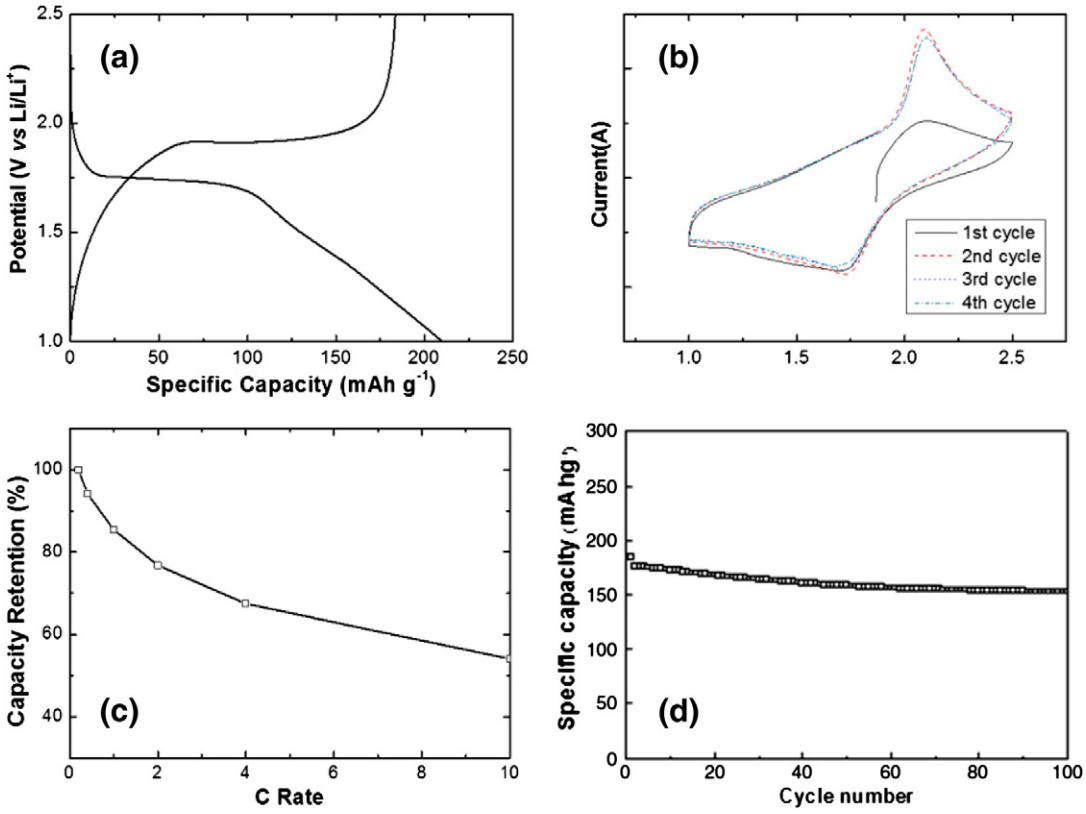

Fig. 3. (a) Initial galvanostatic charge–discharge profiles of CDTN sample at 0.2C; (b) Cyclic voltammogram of CDTN sample in the voltage range of 1.0–2.5 V; (c) Rate capability evaluation with an increase of C rate from 0.2C to 10C; (d) Cycle performance upon 100 cycles at 0.2C.

interconnected carbon phase, facile electrolyte penetration through mesopores and short Li^+ diffusion length within uniform TiO_2 nanocrystals. In Fig. 3(d), the cycle performance is shown within 100 cycles at 0.2C. CDTN anode exhibited stable cycle life with ~83% capacity retention after 100 cycles. When compared with pure TiO_2 nanoparticles showing initial abrupt capacity decay (30% after 10 cycles), our CDTN showed a highly improved cycle performance [8]. This advance of cycle ability was certainly relevant to alleviated nanocrystal aggregation by decorated carbon phase and decrease of structural stress during charging/discharging by the buffer space within mesopores in CDTN.

4. Conclusion

In conclusion, novel interconnected carbon-decorated titania nanocrystals were successfully prepared by direct synthesis route. When applied into anode in lithium ion batteries, outstanding performance improvements were observed, which was attributed to the characteristic crystallographic and morphological structure of the prepared composite material.

References

[1] M.V. Reddy, G.V. Subba Rao, B.V.R. Chowdari, Chem. Rev. 113 (2013) 5364–5457.
[2] A.S. Arico, P. Bruce, B. Scrosati, J.M. Tarascon, W. Van Schalkwijk, Nat. Mater. 4 (2005) 366–377.
[3] Z. Chen, I. Belharouak, Y.-K. Sun, K. Amine, Adv. Funct. Mater. 23 (2013) 959–969.
[4] S.Y. Huang, L. Kavan, I. Exnar, M. Grätzel, J. Electrochem. Soc. 142 (1995) L142–L144.
[5] D. Deng, M.G. Kim, J.Y. Lee, J. Cho, Energy Environ. Sci. 2 (2009) 818–837.
[6] J.W. Kang, D.H. Kim, V. Mathew, J.S. Lim, J.H. Gim, J. Kim, J. Electrochem. Soc. 158 (2011) A59–A62.
[7] X. Su, Q. Xu, X. Zhan, J. Wu, S. Wei, Z. Guo, J. Mater. Sci. 47 (2012) 2519–2534.
[8] H. Liu, L.J. Fu, H.P. Zhang, J. Gao, C. Li, Y.P. Wu, H.Q. Wu, Electrochem. Solid-State Lett. 9 (2006) A529–A533.
[9] L.J. Fu, H. Liu, H.P. Zhang, C. Li, T. Zhang, Y.P. Wu, H.Q. Wu, J. Power Sources 159 (2006) 219–222.
[10] Y. Zhou, Y. Kim, C. Jo, J. Lee, C.W. Lee, S. Yoon, Chem. Commun. 47 (2011) 4944–4946.
[11] M.G. Choi, Y.-G. Lee, S.-W. Song, K.M. Kim, J. Power Sources 195 (2010) 8289–8296.
[12] F.-F. Cao, X.-L. Wu, S. Xin, Y.-G. Guo, L.-J. Wan, J. Phys. Chem. C 114 (2010) 10308–10313.
[13] L. Lu, Y. Zhu, F. Li, W. Zhuang, K.Y. Chan, X. Lu, J. Mater. Chem. 20 (2010) 7645–7651.
[14] T. Yu, Y. Deng, L. Wang, R. Liu, L. Zhang, B. Tu, D. Zhao, Adv. Mater. 19 (2007) 2301–2306.
[15] Y. Zhou, J. Lee, C.W. Lee, M. Wu, S. Yoon, ChemSusChem 5 (2012) 2376–2382.
[16] T. Kemmitt, N.I. Al-Salim, G.J. Gainsford, A. Bubendorfer, M. Waterland, Inorg. Chem. 43 (2004) 6300–6306.
[17] A.L. Patterson, Phys. Rev. 56 (1939) 978–982.
[18] Y. Zhou, C. Jo, J. Lee, C.W. Lee, G. Qao, S. Yoon, Microporous Mesoporous Mater. 151 (2012) 172–179.
[19] M.A. Reddy, M.S. Kishore, V. Pralong, U.V. Varadaraju, B. Raveau, Electrochem. Solid-State Lett. 10 (2007) A29–A31.
[20] Y.-S. Hu, L. Kienle, Y.-G. Guo, J. Maier, Adv. Mater. 18 (2006) 1421–1426.
[21] Y. Ren, L.J. Hardwick, P.G. Bruce, Angew. Chem. Int. Ed. 49 (2010) 2570–2574.
[22] L. Zeng, C. Zheng, L. Xia, Y. Wang, M. Wei, J. Mater. Chem. A 1 (2013) 4293–4299.
[23] Z. Wang, X.W. Lou, Adv. Mater. 24 (2012) 4124–4129.
[24] P. Chang, C. Huang, R. Doong, Carbon 50 (2012) 4259–4268.
[25] B. Li, Z. Zhao, F. Gao, X. Wang, J. Qiu, Appl. Catal. B Environ. 147 (2013) 958–964.
[26] D. Wang, D. Choi, J. Li, Z. Yang, Z. Nie, R. Kou, D. Hu, C. Wang, L.V. Saraf, J. Zhang, I.A. Aksay, J. Liu, ACS Nano 3 (2009) 907–914.
[27] D. Li, D. Shi, Z. Liu, H. Liu, Z. Guo, J. Nanopart. Res. 15 (2013) 1647.